Vanadium centers in ZnTe crystals. II. Electron paramagnetic resonance

J. Kreissl and K. Irmscher
Arbeitsgruppe Elektron-Paramagnetische-Resonanz am Institut für Festkörperphysik, Technische Universität Berlin, Rudower Chaussee 5, D-12484 Berlin, Germany

P. Peka, M. U. Lehr,* and H.-J. Schulz
Fritz-Haber-Institut der Max-Planck-Gesellschaft, Faradayweg 4-6, D-14195 Berlin, Germany

U. W. Pohl
Institut für Festkörperphysik, Technische Universität Berlin, PN 5-1, Hardenbergstraße 36, D-10623 Berlin, Germany
(Received 24 July 1995)

Four V-related electron-paramagnetic-resonance (EPR) spectra are observed in Bridgman-grown ZnTe doped with vanadium. Two of them are attributed to the charge states $V_{Zn}^{3+}(A^+)$ and $V_{Zn}^{2+}(A^0)$ of the isolated V impurity. For the ionized donor, $V_{Zn}^{3+}(A^+)$, the spectrum reveals the typical behavior of the expected $^3A_2(F)$ ground state in tetrahedral symmetry. The incorporation on a cation lattice site could be proved by the resolved superhyperfine interaction with four Te ions. The second spectrum showing triclinic symmetry and $S=\frac{3}{2}$ is interpreted as the neutral donor state $V_{Zn}^{2+}(A^0)$. The origin of the triclinic distortion of the cubic (T_d) crystal field could be a static Jahn-Teller effect. The two additionally observed EPR spectra are attributed to nearest-neighbor V-related defect pairs. The spectrum of the first one, V_{Zn}^{2+}-Y_{Te}, shows trigonal symmetry and can be explained by the $S=\frac{3}{2}$ manifold of an orbital singlet ground state. An associated defect "Y_{Te}" is responsible for the trigonal distortion of the tetrahedral crystal field of V_{Zn}^{2+}. The spectrum of the second pair defect also shows trigonal symmetry and can be described by $S=\frac{1}{2}$. The ground-state manifold implies a V_{Zn}^{3+}-X_{Te} pair as the most probable origin of this spectrum. The $S=\frac{1}{2}$ ground state is produced by a dominating isotropic exchange interaction coupling the $S=1$ ground-state manifold of V_{Zn}^{3+} to an assumed $S=\frac{1}{2}$ ground state of "X_{Te}" in antiferromagnetic orientation. The nature of the associated defects "Y_{Te}" and "X_{Te}" remains unknown for both pairs since no hyperfine structure has been observed, but most probably acceptorlike defects are involved.

I. INTRODUCTION

In most semiconductors, $3d$ transition metals are well known as deep impurities, generally possessing multiple charge states, which strongly influence the electrical and optical material properties. During the past years the investigation of V-related centers in II-VI semiconductors has gained a renewed interest, especially stimulated by the photorefractive behavior of V doped CdTe (e.g., Refs. 1 and 2) and, more recently, that of ZnTe:V,[3] viz., in wavelength regions where semiconductor laser and fiber-optics communications work.

For $3d^n$ elements, including vanadium, it is generally accepted that they preferentially occupy cation lattice sites. The charged donor state of vanadium, $V_{Zn}^{3+}(A^+)\{3d^2\}$, has been verified by electron-paramagnetic resonance (EPR) in ZnS,[4] ZnTe,[5] and ZnSe.[6] Here and in the following, the centers are characterized by the oxidation state $(n+)$ of the defect, as determined by EPR and optical spectroscopy, as well as by the net charge of the defect in the lattice characterized by $A^{(x)}$. Recently, this charge state has also been independently identified in CdTe by at least three groups (Ref. 7, and references therein). All results confirm the cubic symmetry and a $^3A_2$ ground state, which is responsible for the EPR spectrum. So far, the neutral charge state, $V_{Zn}^{2+}(A^0)\{3d^3\}$, could only be observed in ZnS.[8] In that case, the spectrum was recorded at 77 K and interpreted as a trigonally distorted V^{2+} center. A $T\otimes\tau_2$ Jahn-Teller (JT) effect should be responsible for the trigonal distortion. Compared with other tetrahedrally coordinated $3d^3$ ions exhibiting a symmetry lowering ascribed to the JT effect, the temperature at which the spectrum had been observed was unusually high. For the isoelectronic charge state Cr^{3+} in GaAs, an orthorhombic EPR spectrum was reported.[9,10] The spectrum could only be detected at temperatures below 10 K. The origin of the orthorhombic distortion should be a strong JT effect involving both τ_2 and ϵ vibronic modes (anharmonic terms and/or nonlinear JT coupling).[11,12] Very recently, a triclinic V-related spectrum has been verified in CdTe that is attributed to $V_{Cd}^{2+}(A^0)$.[13] In a preliminary note, a V-related spectrum in $Cd_{(1-x)}Zn_xTe$ was also tentatively assigned to $V_{Cd}^{2+}(A^0)$.[14] $V_{Zn}^{+}(A^-)\{3d^4\}$ could not yet be observed by EPR, although evidence for its occurrence was found by optical spectroscopy in ZnS and ZnSe.[15]

The optical properties of V-doped II-VI compounds have been investigated for a long time, verifying transitions attributed to $V^{3+}(A^+)$, $V^{2+}(A^0)$, and $V^{+}(A^-)$. The vanadium ion thus proves to be an amphoteric impurity (Refs. 16 and 17 and references therein). Compared with ZnS and ZnSe, the knowledge about vanadium-related defects in ZnTe is not very comprehensive. In part I of this paper, the three charge states of isolated vanadium (3+, 2+, +) placed on Zn sites could be verified by their luminescence transitions. The broad emission bands display weak no-phonon lines near 4726 cm^{-1} [$^3T_2(F)\rightarrow{}^3A_2(F)$ transition of $V_{Zn}^{3+}(A^+)$

$\{3d^2\}$], 4056 cm^{-1} [$^4T_2(F) \rightarrow {}^4T_1(F)$ of $V_{Zn}{}^{2+}(A^0)$ $\{3d^3\}$] and 3401 cm^{-1} [$^5E(D) \rightarrow {}^5T_2(D)$ of $V_{Zn}{}^{+}(A^-)$ $\{3d^4\}$]. Excitation spectra could be separately recorded for these three bands and are analyzed in terms of the respective excited states and the related charge-transfer transitions. Further luminescence peaks were tentatively attributed to V-related complexes, probably those which will be discussed by the EPR studies in the second paper.

To complete the optical data, we have studied the ground states of the V-related defects in ZnTe:V single crystals by EPR. Four different V-related spectra could be detected, two of them are related to the isolated V defects observed also in part I by optical studies and the two others are assigned to V-related complexes.

II. EXPERIMENT

The ZnTe:V bulk crystals used in this study are the same as described in part I. {110} cleavage planes were chosen as rotation planes in the magnetic field. The EPR spectra were recorded in the *X* (9.44 GHZ) and *Q* (34.0 GHz) bands using a Bruker ESP300E spectrometer equipped with Oxford He gas-flow cryostats. Illumination of the samples with a halogen lamp was possible during the EPR experiments.

III. RESULTS AND DISCUSSION

Typical EPR spectra of ZnTe:V crystals prove (Fig. 1) in all cases the incorporation of vanadium by its characteristic eightfold hyperfine structure of the EPR lines, due to the magnetic electron-nuclear interaction at the isotope ^{51}V with a nuclear spin $I=\frac{7}{2}$ and a natural abundance of 99.75%. In the spectra for the magnetic-field orientation parallel to a $\langle 110\rangle$ crystal axis at 4 K [Fig. 1(a)] and at 20 K for $B \| \langle 100\rangle +10°$ [Fig. 1(b)], besides the V-related defects, which shall be discussed below, spectra of the unintentionally incorporated transition metals $Mn_{Zn}{}^{2+}$ and $Co_{Zn}{}^{2+}$ in the dark and $Fe_{Zn}{}^{+}$ under band-gap illumination are detected [Fig. 1(b)]. The V-related spectra are not photosensitive. The analysis of the V-related spectra in the following sections is based on the usual description by an appropriate spin Hamiltonian (SH), which, in the present case, turns out to be of the form

$$\mathcal{H}=\mathcal{H}_Z+\mathcal{H}_F+\mathcal{H}_{HF}+\mathcal{H}_{SHF},$$

$$\mathcal{H}_Z=\beta\sum_{i=x,y,z} g_i B_i S_i,$$

$$\mathcal{H}_F=D[S_z^2-\tfrac{1}{3}S(S+1)]+E(S_x^2-S_y^2), \qquad (1)$$

$$\mathcal{H}_{HF}=\sum_{i=x,y,z} A_i^V S_i I_i^V,$$

$$\mathcal{H}_{SHF}=\sum_{i=1}^{4}\sum_{j=\xi_i,\eta_i,\zeta_i} A_j^{Te} S_j I_j^{Te},$$

including the Zeeman interaction $\mathcal{H}_z$, the electronic quadrupole interaction $\mathcal{H}_F$ (fine structure), the electron-nuclear hyperfine interaction with the nuclear spin of vanadium $\mathcal{H}_{HF}$, and the electron-nuclear superhyperfine interaction with all nuclear spins *i* of the ligands appreciably interacting with the electronic spin $\mathcal{H}_{SHF}$. Not all of the occurring SH parameters could be determined for each of the four V-related centers, because of too low experimental resolution (mainly caused by overlapping lines) or since some of them were zero according to the observed spin states and symmetries.

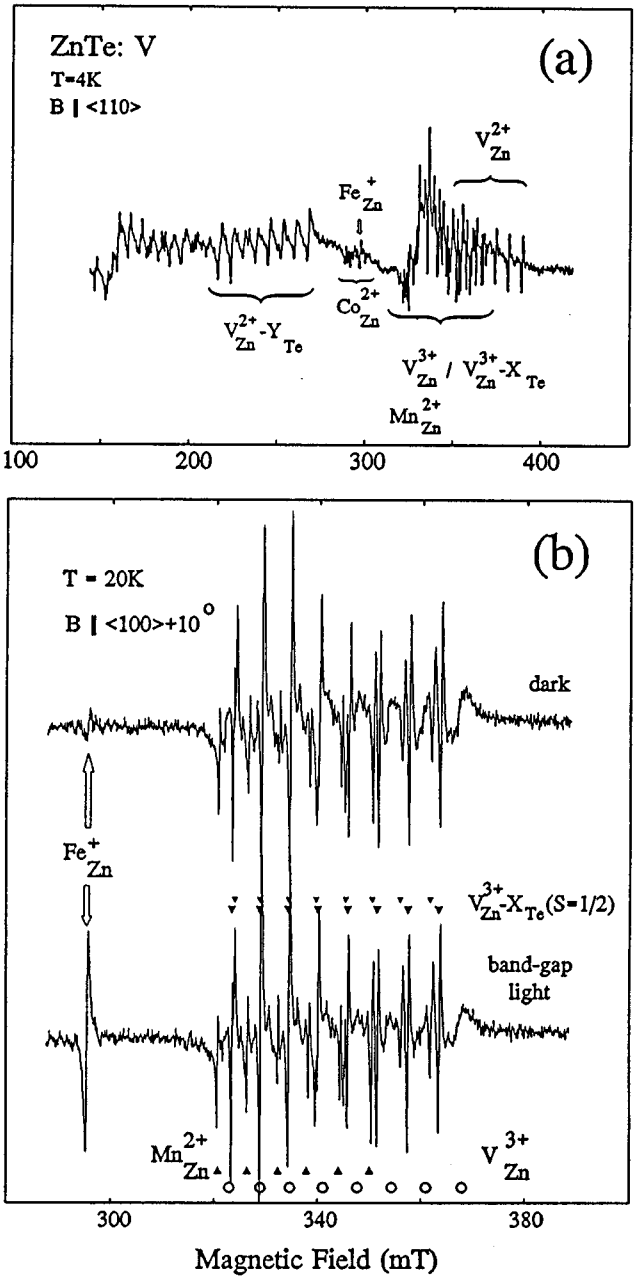

FIG. 1. *X* band EPR spectra of ZnTe:V for (a) a measurement at 4 K in the dark and (b) at 20 K in the dark (top) and under the influence of band-gap illumination (bottom).

A. Isolated V centers: $V_{Zn}{}^{3+}(A^+)$ and $V_{Zn}{}^{2+}(A^0)$

At low microwave power an eightfold split, isotropic spectrum was observed between 4 and 70 K. Except the high-field line all other hyperfine transitions are superimposed by other spectra. Contrary to the common EPR experience in II-VI semiconductors, the lines are very broad

TABLE I. Spin-Hamilton parameters of the isolated $V_{Zn}^{3+}(A^+)$ $\{3d^2\}$ impurity in ZnTe with cubic symmetry.

S	g	$\lvert A^V\rvert$ (10^{-4} cm^{-1})	$\lvert A^{Te}\rvert$ (10^{-4} cm^{-1})	Refs.
1	1.917[a]	57.8	-	5
1	1.959 (1)	57.6 (5)	first shell $\lvert A_{\parallel}^{Te}\rvert = 44.0$ (5)	this paper
			$\lvert A_{\perp}^{Te}\rvert = 17.0$ (5)	
			third shell $\lvert A^{Te}\rvert = 1.1$ (1)	

[a]We do not realize the reason for the difference in the g values, but we do not believe in the occurrence of two different centers.

($\Delta B_{pp}=2.8$ mT). With increasing microwave power, sharp signals ($\Delta B_{pp}=0.04$ mT) grow up from each broad hyperfine line. These sharp signals show a further splitting, due to the interaction with nuclear spins of the surrounding host ions (superhyperfine interaction).

Such a behavior of a spectrum has been repeatedly observed for $3d^2$ ions in II-VI semiconductors (Refs. 4 and 7, and references therein). ZnTe:V_{Zn}^{3+} was briefly reported by Woodbury and Ludwig.[5] The tetrahedral crystal field at the cation site splits the ^3F ground state of the free V^{3+} ion into the terms $^3T_1(F)$, $^3T_2(F)$, and $^3A_2(F)$, in order of decreasing energy. The EPR transitions were observed within the $S=1$ spin triplet of the $^3A_2(F)$ ground state. Using the SH (1) for the description of the spectrum, only a reduced set of parameters is necessary if one bears in mind that in pure T_d symmetry, there is no fine-structure splitting, i.e., $D=E=0$, and the Zeeman as well as the hyperfine interaction are isotropic and can be described by g and A^V, given in Table I. The parameters were fitted using third-order perturbation theory for the hyperfine interaction. The lower-than-cubic symmetry at the ligand sites implies an anisotropic superhyperfine interaction. Indeed, the superhyperfine structure of the double-quantum transitions reveals trigonal symmetry (Fig. 2) and is, therefore, assigned to the four Te ions of the first shell. This is in line with the behavior of other transition-metal impurities in several II-VI compounds.[18] The angular dependence the superhyperfine structure can be calculated by four equivalent Te nuclei taking into account that ^{125}Te is the only isotope with an appreciable natural abundance (6.99%), which has a nonzero nuclear spin ($I=\frac{1}{2}$) and is shown by solid lines in Fig. 2 using the parameter of the first shell $A_{\parallel}^{Te}$ and $A_{\perp}^{Te}$. The slight deviations between experimental and calculated line positions as well as the in some cases additional line splitting of the spectra (Fig. 2) are caused by a small misalignment of the $\langle 110\rangle$ rotation axis. With a further decrease of the modulation amplitude, an isotropic three-line structure becomes observable on the central line (CL) (Fig. 2). The best fit of this structure was achieved under the assumption of the interaction with the third shell of twelve Te ions using a Lorentzian line shape of a width of $\Delta B_{pp}=0.036$ mT and the superhyperfine parameter A^{Te} also given in Table I. The isotropic lines, marked by $*$ in Fig. 2, have not been considered so far. Their origin might be the unresolved superhyperfine interaction with twelve Zn ions of the second shell. The incorporation of V on a Zn site is thus proved since (i) this structure clearly differs from that calculated for a V ion fourfold coordinated by Zn, and (ii) an interstitial site of V is very unlikely, because the observed spin state is consistent with the electronic structure of a substitutional site.

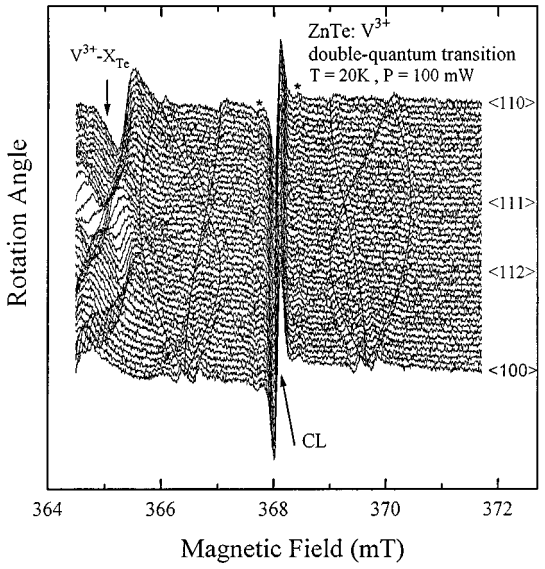

FIG. 2. Angular dependence of the superhyperfine structure of one hyperfine transition of $V_{Zn}^{3+}(A^+)$ for experimental conditions, where the double-quantum transition is dominating the single-quantum transitions (stack plot) and calculated angular dependence (solid lines) of the interaction, with the four Te ions of the first shell. The magnetic field is rotated in the {110} plane. The further splitting of the central line (CL) and the transitions marked by $*$ are interpreted as the interaction with the third and second shell. Details are given in the text.

The described two kinds of EPR transitions are yielded by two superimposed single quantum transitions $|1\rangle \rightleftarrows |0\rangle$ and $|0\rangle \rightleftarrows |-1\rangle$ (broad signal) and one double-quantum transition $|1\rangle \rightleftarrows |-1\rangle$ (sharp signal), viz., the simultaneous absorption of two microwave quanta. This conclusion could be verified by the different power dependence of the two types of transitions (e.g., Ref. 7 and references therein). The reason for the broadening are random strains which reduce the individual symmetry of the defect accidentally and, therefore, lift partially the threefold spin degeneracy, thus producing a singlet and a doublet. The single-quantum transitions occur between the singlet and the doublet states and, therefore, the line positions are directly influenced leading to a broadening. The double-quantum transition occurs only between the doublet states, which are unaffected by random-strain splitting, and the line remains sharp. The large difference in the linewidths between the two types of transitions indicates the occurrence of remarkable random strains in the crystal.

Within the framework of simple crystal-field theory, the g value shows the shift typical for a $^3A_2$ ground state in a T_d crystal field. According to the relation[19] $g=g_e-8k\lambda_0/\Delta$, we get an exceptionally small value $k=0.25$ (implying an unusual large covalency) for the covalency reduction factor if we use $g_e=2.0023$ as the free-electron value, $\lambda_0=104$ cm^{-1} as the spin-orbit coupling constant of the free V^{3+} ion,[19] and $\Delta=10Dq$ as the energy difference between the $^3T_2(F)$ and $^3A_2(F)$ states, recently measured by luminescence[(part I)] as $\Delta=4726$ cm^{-1}. The k value in ZnTe is similar to that determined for $V_{Zn}^{3+}(A^+)$ in CdTe.[7]

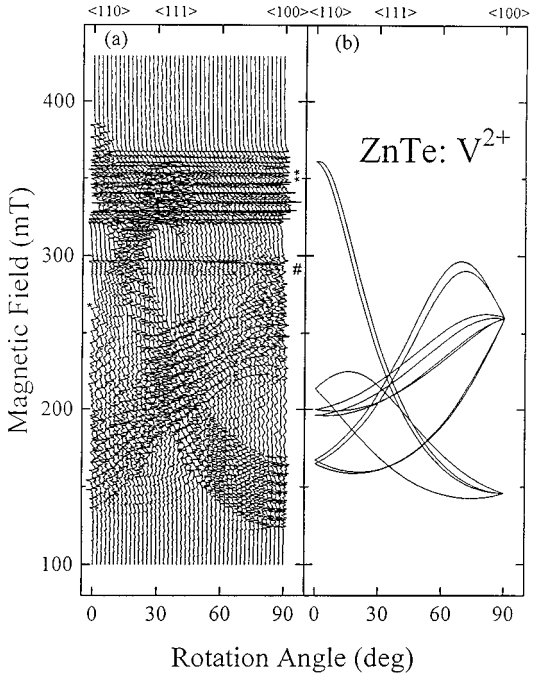

FIG. 3. Angular dependence of the ZnTe:V EPR signal at 4 K in the X band. Stack plot of the EPR spectra (a) and a plot of the calculated fine-structure line positions for the triclinic $V^{2+}(A^0)$ impurity (b). The magnetic field is rotated in a {110} crystal plane. Those EPR lines, which do not belong to the V^{2+} are marked by ** for superposition of $V^{3+}(A^+)$, the trigonal $V_{Zn}{}^{3+}-X_{Te}$ pair, and residual $Mn^{2+}(A^0)$, by * for the trigonal $V_{Zn}{}^{2+}-Y_{Te}$ pair, and by # for residual $Fe^{+}(A^-)$ and $Co^{2+}(A^0)$.

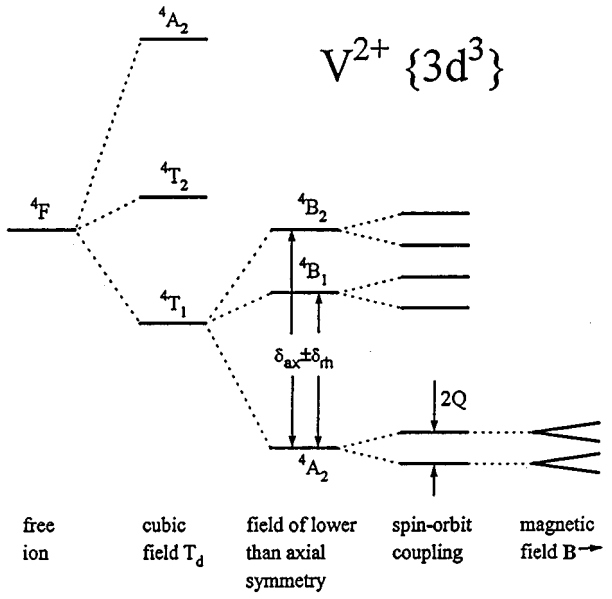

FIG. 4. Schematic term splitting of the ground state of V^{2+} $\{3d^3\}$ in a T_d crystal field including low-symmetry distortions and spin-orbit coupling.

Furthermore, we observe a second V-related spectrum assigned to the isolated $V_{Zn}{}^{2+}(A^0)$ (Figs. 1 and 3). The simultaneous occurrence of the neutral charge state, $V_{Zn}{}^{2+}(A^0)$, with the already described positive charge state A^+ is expected if the Fermi level is pinned at the V donor level. In a tetrahedral crystal field, the orbital triplet $^4T_1$, which is split off from the free-ion ground state ^4F of V^{2+}, is lowest in energy (see Fig. 4). If there are no other distortions lifting the orbital degeneracy, such a ground state is known to undergo a JT effect which, in its static limit, lowers the symmetry of the (static) crystal field at the impurity ion site.

The linewidth of each of the eight hyperfine transitions of the $V_{Zn}{}^{2+}(A^0)$ spectrum is about 0.5 mT. Therefore, it is not surprising that the expected superhyperfine splitting, due to the *Te* ligands, cannot be observed in contrast to the case of the sharp double-quantum transition lines of $V_{Zn}{}^{2+}$. Furthermore, it should be mentioned that no additional line splitting, due to a nearby symmetry-lowering impurity (see below) abundant with nonzero nuclear spin, could be resolved. When the temperature of the sample is raised above 12 K, there is a rapid decrease in the observability of the lines. The experimental angular dependence of the EPR lines and the calculated $V_{Zn}{}^{2+}(A^0)$ dependence, neglecting the hyperfine splitting for clarity, are shown in Fig. 3 for a rotation in a {110} plane. This pattern indicates triclinic symmetry, but with only a small deviation of the quantization axis z from a ⟨110⟩ crystalline direction. As mentioned above, such a lowering from tetrahedral symmetry is not surprising. It splits the orbital triplet $^4T_1$ into three orbital singlets, each one with fourfold spin degeneracy, which is partially lifted by the spin-orbit coupling finally leaving six Kramers doublets (Fig. 4). The energetic splittings arising from the latter two interactions are of such an order of magnitude that at low temperatures an appreciable occupation can only be expected for the lowest two doublets, which will be referred to in the following as the ''lower'' and the ''upper'' Kramers doublets. The analysis of the spectrum with SH (1) and $S=3/2$ shows that our observations of spin transitions are restricted to the lower doublet, because the zero-field splitting $2Q=2(D^2+3E^2)^{1/2}$ is large enough to prevent transitions between both Kramers doublets (in spite of their high transition probability and Q-band employment) and within the upper one as well (because of insufficient thermal occupation). There are several additional reasons rendering difficult a precise determination of the SH parameters (g, D, E, A_i^V) and of the principal axes of the center system (x, y, z): (i) triclinic point symmetry in a crystal of T_d symmetry results in 24 center orientations, only for an exact {110} rotation plane reduced to 12 magnetically nonequivalent orientations, corresponding in our case to at least 12 EPR lines (neglecting hyperfine interaction) for each arbitrary angle of the rotation pattern; (ii) considerable spreading of the spectrum due to the strong hyperfine interaction with the ^{51}V nucleus; and (iii) strong overlapping by other spectra. Fortunately, a description of the angular dependence of the spectrum is possible by an effective spin $S'=\frac{1}{2}$ dropping all terms of SH (1), but that of the Zeeman interaction, now with effective g values g_i'. This approximation requires that the zero-field splitting $2Q$ be large compared to the Zeeman splitting (or the microwave quantum $h\nu$), as already concluded from the missing transitions to and within the upper doublet. Taking into account this experimental fact, a lower limit of $2Q$ is roughly estimated as about 10 cm^{-1}. Bearing in mind the experimental difficulties, the rotation pattern [Fig. 3(b)] can be fitted by the effective g values and

TABLE II. Spin-Hamilton parameters of the isolated $V_{Zn}^{2+}(A^0)$ $\{3d^2\}$ impurity in ZnTe with triclinic symmetry; $\{(z,y,x)$ are the principal axes with $z\|[-0.019, 0.702, 0.712]$, $y\|[0.962, -0.18, 0.204]$, and $x\|[-0.271, -0.689, 0.672]\}$, and z', y', x' are parallel to [011], [100], [011], respectively}.

(a) Effective spin $S'=\frac{1}{2}$ description						
$S'=\frac{1}{2}$	$g'_{z'z'}$	$g'_{y'y'}$	$g'_{x'x'}$	$g'_{x'y'}$	$g'_{x'z'}$	$g'_{y'z'}$
	1.869 (5)	4.60 (5)	3.13 (5)	0.45 (10)	0	0.05 (3)
	g'_z	g'_y	g'_x			
	1.868 (5)	4.73 (5)	3.00 (5)			
(b) $^4A_2$ ground state						
$S=\frac{3}{2}$	g_z	g_y	g_x			
	2.0023	1.96 (5)	1.97 (3)		$E/D=0.153$ (3)	
^{51}V hyperfine parameter (10^{-4} cm^{-1})		$\|A\|$				
		60 (2)				

the principal axes given in Table II. To link the effective g values with the SH parameters in the description of the spectrum by the real spin $S=\frac{3}{2}$, at first the fine-structure term of the SH (1) is diagonalized within the manifold of the spin quartet and then the first-order Zeeman corrections are calculated yielding the well-known formula, e.g., Ref. 20:

$$g'_x=g_x[1-(3E-D)/Q],$$
$$g'_y=g_y[1+(3E+D)/Q], \qquad (2)$$
$$g'_z=g_z(2D/Q-1), \quad Q=\sqrt{D^2+3E^2},$$

valid for the lower doublet, which we could determine for the three principal g' values. Since Eq. (2) contains four unknowns (g_x, g_y, g_z, and E/D), it can only be solved unambiguously if an assumption is made for at least one of them. Following Hennig, Liebertz, and van Stapele,[20] g_z was fixed at the free-electron value $g_e=2.0023$. The obtained SH parameters are summarized for $S=\frac{3}{2}$ in Table II. The fine-structure constant D itself remains undetermined, except that it is positive and exceeds a lower limit as discussed above.

To check in more detail our assumption of a triplet orbital ground state $^4T_1$ split by the action of a crystal field of lower symmetry than cubic and spin-orbit coupling, a Hamiltonian is used that treats the ground-state manifold by a fictitious orbital momentum $l'=1$ and the real spin $S=\frac{3}{2}$. It can be written[21] (using the signs of Ref. 19)

$$\mathscr{H}=\delta_{ax}[l'^2_z-\tfrac{1}{3}l'(l'+1)]+\delta_{rh}(l'^2_x-l'^2_y)+\alpha\lambda\sum_{i=x,y,z}l'_iS_i, \qquad (3)$$

where we have denoted the axial field component (direction of z) by δ_{ax}, the rhombic component by δ_{rh}, the effective orbital Landé factor by α (restriction to a single one), and the spin-orbit coupling constant by λ. Taking $\alpha=-1$, the limit for a strong cubic field, the Hamiltonian (3) can be diagonalized in first approximation. The dependences of the resulting energy eigenvalues on the axial field component were calculated in units of λ. With the corresponding eigenstates and the Zeeman Hamiltonian,

$$\mathscr{H}_z=\beta\sum_{i=x,y,z}(g_eB_iS_i-\alpha B_il'_i), \qquad (4)$$

appropriate for the treated model, the first-order Zeeman splitting can be determined and related to the principal g' values. The best approximation to the experimentally determined effective g values is obtained for $\delta_{ax}/\lambda=69$ and $\delta_{rh}/\delta_{ax}=0.15$. The fine-structure splitting of the two lowest Kramers doublets amounts to $2Q/\lambda=0.03$ at this point, which renders only $2Q\approx1.7$ cm^{-1} taking $\lambda=55$ cm^{-1}, the spin-orbit coupling constant of the free ion V^{2+}. Though this value of $2Q$ is by at least a factor of 6 too small compared to our observations, this simple model supports the assumption concerning the ground state within the cubic field. Furthermore, one can conclude that the sign of the z component δ_{ax} of the triclinic field distortion must be positive with the orbital singlet $^4A_2$ lowest in energy, because in the opposite case with a ^4B term lowest, though yielding similar g' values, the order of both Kramers doublets is reversed, in contrast to that implied by the experiment.

The similarity to the isoelectronic Cr^{3+} center[9,10] in particular the temperature range where the signals appear, lets us conclude that the origin of the triclinic symmetry of the $V_{Zn}^{2+}(A^0)$ center is a static JT effect and not an associated defect as in the cases discussed in Sec. III B. The JT effect is in its static limit, as can be inferred from the large line intensity, and leads to a C_{2v} symmetry. The lowering from C_{2v} to C_1 is possibly due to a weak off-center shift of $V_{Zn}^{2+}(A^0)$. Whether such an additional distortion is present also for Cr^{3+} in GaAs cannot be decided as the linewidth of the EPR transitions in GaAs:Cr^{3+} is larger by a factor of 20 compared with ZnTe:V^{2+}.

B. V-related pair defects

In addition to the two spectra which have been assigned to the neutral and positive effective charge states of the isolated V impurity in ZnTe, two further V-related spectra could be verified in a temperature range between 4 and 70 K. Parts of these spectra, designated $V_{Zn}^{2+}-Y_{Te}$ and $V_{Zn}^{3+}-X_{Te}$, are also shown in Figs. 1 and 3. For the first one, the angular dependence of the fine structure is shown in Fig. 5, for mea-

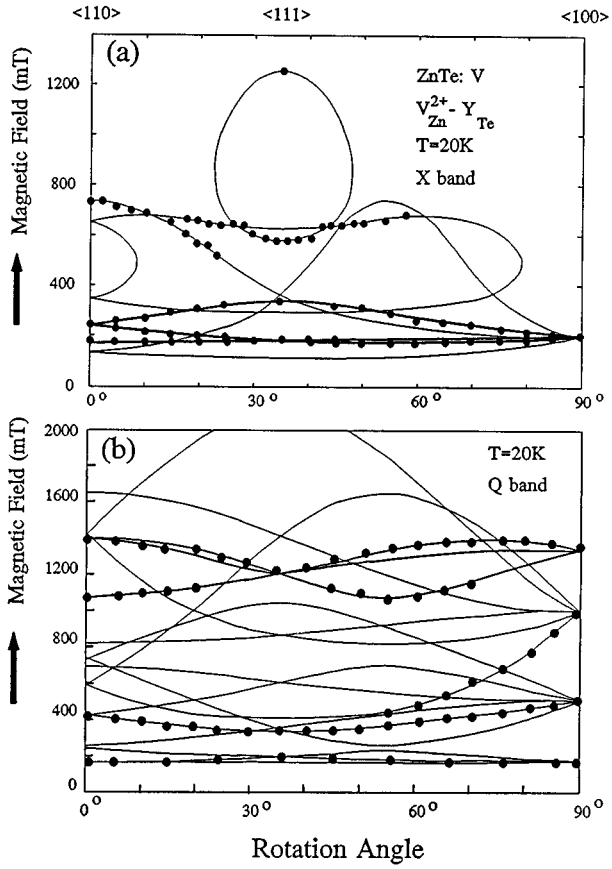

FIG. 5. Trigonal angular dependence of the fine-structure line positions of the $V_{Zn}{}^{2+}-Y_{Te}$ pair in ZnTe obtained in the X band (a) and the Q band (b). The magnetic field is rotated in a {110} plane. The experimental data are plotted as solid circles.

surements in the X band, as well as in the Q band, and indicates trigonal symmetry. For the X band, the most intensive groups of transitions occur in the low-field range between 150 and 350 mT [bold lines in Fig. 5(a)], a situation which is characteristic of a spin system with an odd number of unpaired electrons in the weak-magnetic-field limit ($D \gg h\nu_{\mathrm{MW}}$). In the weak-magnetic-field approximation, the lines can be described with an effective spin $S'=\frac{1}{2}$ and $g'_{\parallel}=2.000$, $g'_{\perp}=3.83$. This behavior is expected for transitions within a $|\pm\frac{1}{2}\rangle$ doublet of a spin-$\frac{3}{2}$ system, with a large trigonal zero-field splitting, where the effective g values become $g'_{\parallel}=2$ and $g'_{\perp}=4$. Therefore, we assigned this spectrum with $S=\frac{3}{2}$ to a $V_{Zn}{}^{2+}(A^0)$-related defect, for which the ground state behavior is determined by the $3d^3$ electrons of the V ion implying a spin of $\frac{3}{2}$. As mentioned in Sec. III A, $V_{Zn}{}^{2+}(A^0)$ has an orbitally degenerate $^4T_1$ ground state, in T_d symmetry split by the trigonal distortion into an orbital singlet $^4A_2$ and an orbital doublet ^4E. The fourfold spin degeneracy of the $^4A_2$ ground state is partially lifted by spin-orbit coupling into two Kramers doublets. *A priori*, we cannot decide whether the origin of the observed trigonal distortion is caused by a JT effect or an associated defect, but we claim that an associated defect "Y_{Te}" is responsible for the lowering of symmetry in the present case. The main argument for the occurrence of an associated defect "Y_{Te}" stems from the fact that the spectrum is measurable without line broadening up to 70 K, which is more typical for pair defects than for JT behavior (compare, e.g., the triclinic $V_{Zn}{}^{2+}(A^0)$ center in this paper with the Cr^{3+} center in GaAs, where the spectra disappear for temperatures higher than about 10 K, because of line broadening).

For a trigonal center of $S=\frac{3}{2}$, the energy levels can be described by the Hamiltonian (1), where the z axis of the principal-axes system coincides with the trigonal C_3 symmetry axis parallel to $\langle 111\rangle$. The x and y axes are arbitrarily oriented in the plane perpendicular to z. According to the four C_3 directions, there are four magnetically different center positions, two of which are always magnetically equivalent under rotation around a $\langle 110\rangle$ axis, as employed in our experiments.

However, the deviation of the observed $g'_{\perp}$ value from the limit $g'_{\perp}=4$, and the occurrence of several additional transitions in the high-field region [Fig. 5(a)] suggests that the fine-structure splitting is not totally dominating over the Zeeman splitting in the X-band experiment. To define an initial value for the procedure of exact diagonalization of the energy matrix yielded from the Zeeman and fine-structure parts of (3), we use perturbation theory (e.g., Ref. 22).

$$g'_{\perp}=2g_{\perp}\left(1-\frac{3}{4}\left[\frac{g_{\perp}\beta B}{2D}\right]^2\right). \tag{5}$$

Under the assumption of $g_{\perp}=2$ (confirmed below by the fit of the total angular dependences in X and Q bands), it is straightforward to estimate from Eq. (5) $|D|$ at about 0.4 cm^{-1}, which is in the same order as the Zeeman energies at the resonances. Consequently, an analysis of all fine-structure transitions using perturbation theory is not suitable. In order to proceed in such a case, we have applied the method of direct diagonalization of the $S=\frac{3}{2}$ energy matrix of the Zeeman and fine-structure part of the spin Hamiltonian (1). Starting from the initial spin-Hamilton parameters discussed above, we fit the observed angular fine-structure dependences in the X and Q bands. The parameters of the best fit are given in Table III. To explain the origin of some of the transitions, we have plotted the energy levels of the $S=\frac{3}{2}$ ground-state manifold for the magnetic field parallel ($z\|B$) and perpendicular ($z\perp B$) to the C_3 axis, where D is assumed to be positive (Fig. 6).

The reason for the completely changed pattern in the Q band [Fig. 5(b)] is the altered ratio between the field-independent zero-field splitting characterized by D and the Zeeman splitting, which is about four times larger as in the X band. Indeed, to describe the $|\pm 1/2\rangle$ transitions [bold lines in Fig. 5(b)], we have to swap the common perturbation theory for a treatment where the fine structure is considered as a perturbation of the Zeeman splitting ($D \ll g\beta B$). In that limit, the angular dependence of the electronic $+\frac{1}{2}\leftrightarrow-\frac{1}{2}$ transitions is mostly determined by terms proportional to $D^2/g\beta B$.[19] However, also for the Q band, the demand $D \ll g\beta B$ is not really fulfilled and, therefore, it is necessary to apply the direct diagonalization of the energy matrix. The parameters given in Table III fit also the Q band angular dependence shown in Fig. 5(b).

The hyperfine parameters of Table III were determined by the fitting of the hyperfine line position for $B\|z$ and $B\perp z$

TABLE III. Spin-Hamilton parameter of both trigonal spectra of $V_{Zn}^{3+}-X_{Te}$ and $V_{Zn}^{2+}-Y_{Te}$ pairs in ZnTe ($z\|\langle 111\rangle$).

					^{51}V hyperfine parameter	
Defect	S	$g_\parallel$	$g_\perp$	$\lvert D\rvert$ (cm^{-1})	$\lvert A_\parallel\rvert$ (10^{-4} cm^{-1})	$\lvert A_\perp\rvert$ (10^{-4} cm^{-1})
$V_{Zn}^{3+}-X_{Te}$	$\frac{1}{2}$	1.975 (1)	1.964 (1)		46.4 (5)	53.7 (5)
$V_{Zn}^{3+}-Y_{Te}$	$\frac{3}{2}$	2.000 (5)	2.000 (5)	0.414 (3)	49 (1)	53 (1)

applying perturbation theory. For arbitrary orientation the V hyperfine structure becomes more complicated because of the simultaneous occurrence of allowed ($\Delta m=0$) and forbidden ($\Delta m=\pm 1$) nuclear-spin transitions. In this case, the mixing of nuclear states is caused by the effective magnetic field acting on the V nucleus, which is created by the comparable electronic Zeeman and zero-field splittings.

The analysis of the spectrum has proved that the behavior of the spectrum can be interpreted by a $V_{Zn}^{2+}(A^0)$ ion in a trigonally distorted tetrahedral crystal field. It seems to be most probable that the trigonal distortion is produced by an associated closed-shell defect "Y_{Te}," which occupies the nearest-neighbor Te site.

For the second spectrum discussed in this section, called $V_{Zn}^{3+}-X_{Te}$, the angular dependences are given in Figs. 7(a) and 7(b) for measurements at X and Q band frequencies, respectively. The experimental data were interpolated by continuous lines, which coincide with those obtained by a fit and only these are shown in the figure for clarity. The angular dependences show trigonal symmetry of the defect and can be described by a simple $S=\frac{1}{2}$ spin Hamiltonian including hyperfine interaction (for a $S=\frac{1}{2}$ ground-state manifold the fine-structure term is irrelevant). As discussed above, we expect three magnetically different center positions for a center with trigonal symmetry if we rotate around a $\langle 110\rangle$ crystal

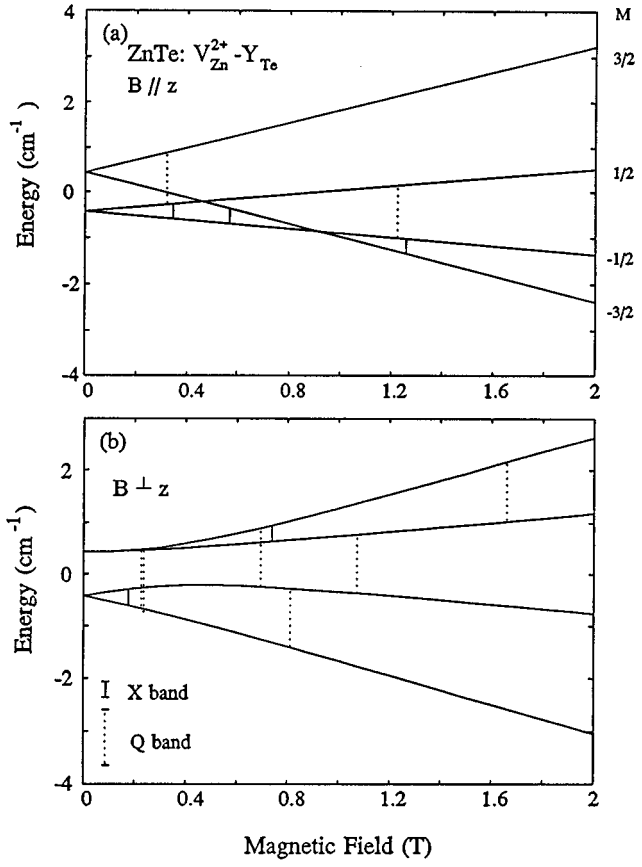

FIG. 6. Energy-level diagram for the $V_{Zn}^{2+}-Y_{Te}$ pair in ZnTe for the magnetic-field oriented parallel (a) and perpendicular (b) to the trigonal axis. EPR transitions at 9.44 GHz (X band) and 34 GHz (Q band) are indicated by solid and dotted lines, respectively. For an exact parallel orientation (a), only allowed $\Delta M=\pm 1$ electronic spin transitions have a transition probability unequal to zero, therefore, only those transitions are included.

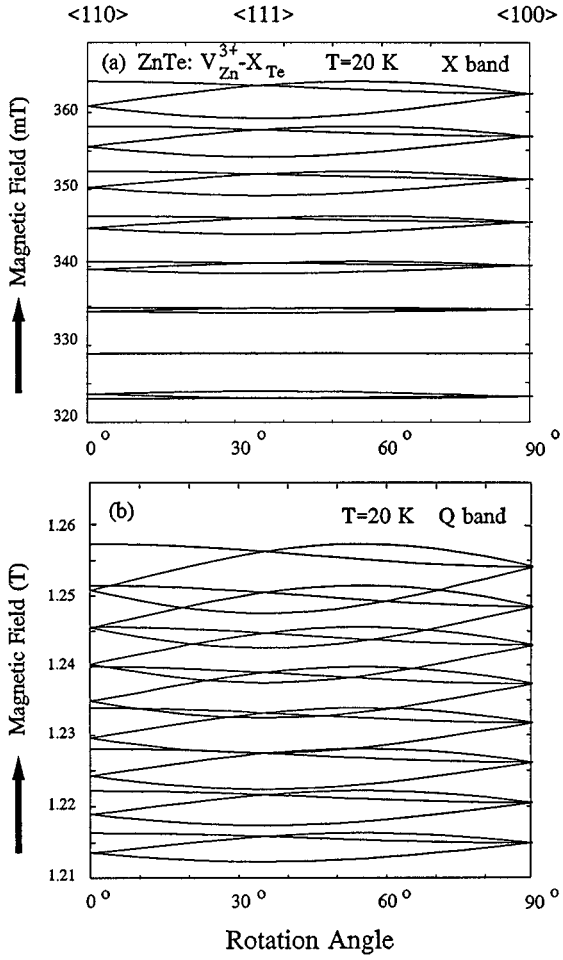

FIG. 7. Angular dependence of the EPR line positions of the trigonal $V_{Zn}^{3+}-X_{Te}$ pair in X-band (a) and Q-band measurements (b) (note here that the hyperfine splitting is taken into account). The magnetic field is rotated in a {110} plane.

axis. The spin Hamiltonian was treated by second-order perturbation theory for $|A|<g\beta B$. The line positions of the allowed $(\frac{1}{2},m)\leftrightarrow(-\frac{1}{2},m)$ transitions were calculated after[19]

$$B_{1/2\leftrightarrow -1/2,m\leftrightarrow m}=B_0-Am-(A_\parallel^2+A^2)\,\frac{A_\perp^2}{4A^2B_0}\times[I(I+1)-m^2]-\left[\frac{(A_\parallel^2-A_\perp^2)^2}{8A^2B_0}\left(\frac{g_\parallel g_\perp}{g^2}\right)^2\sin^2 2\theta\right]m^2, \tag{6}$$

with

$$B_0=\frac{h\nu}{g\beta},$$

$$g^2=g_\parallel^2\cos^2\theta+g_\perp^2\sin^2\theta,$$

$$g^2A^2=g_\parallel^2A_\parallel^2\cos^2\theta+g_\perp^2A_\perp^2\sin^2\theta,$$

where all symbols have their usual meaning (here the HF parameter A is used in magnetic field units). θ is the angle between the magnetic field and the z axis ($z\|C_3$). The spin-Hamilton parameters rendering the best fit are listed in Table III. The g values near 2 and their slight anisotropy verify that $S=\frac{1}{2}$ is the total spin of the ground state and not an effective one, as in the cases discussed for the V^{2+} centers.

In the following, we will give a discussion of the $S=\frac{1}{2}$ ground-state manifold, which is unusual for V-related defects in II-VI materials. For isolated impurities or complexes, where the electronic behavior is determined only by the V ion, a $S=\frac{1}{2}$ spin manifold of the ground state is expected for $V_{Zn}^{4+}(A^{2+})$ $\{3d^1\}$ in its high-spin configuration and for $V_{Zn}^{2+}(A^0)$ $\{3d^3\}$ in its low-spin configuration. The Tanabe-Sugano scheme of $V_{Zn}^{2+}(A^0)$ shows[(part I)] that the possibility of a low-spin behavior might be realistic in the case of a small increase of the crystal-field strength. In both instances a ^2E ground state is expected, which should undergo a JT effect. It is known for an E state that it interacts with the ϵ vibration modes resulting in a tetragonal JT distortion. This expected behavior for E ground states contradicts our observations and furthermore, the existence of a double donor, $V_{Zn}^{4+}(A^{2+})$, in ZnTe is very unlikely. Both remaining V charge states which possibly occur in ZnTe, $V_{Zn}^{3+}(A^+)$ and $V_{Zn}^{+}(A^-)$, have an even number of $3d$ electrons producing a ground-state multiplet with an integer spin and therefore, cannot be responsible for the spectrum.

A type of defect that might be account for the spectrum shall be discussed now. Based on the trigonal symmetry, we suggest a nearest-neighbor pair of V_{Zn} and an associated defect "X_{Te}" at a Te site (Fig. 8). Both defects should be paramagnetic, with a dominating exchange interaction between them. The isotropic exchange interaction can be described by the spin Hamiltonian,[23]

$$\mathscr{H}_{ex}=J_{V,X}S_VS_X. \tag{7}$$

In the strong-exchange limit, we consider the effects of the other spin operators as a perturbation to the eigenvalues of

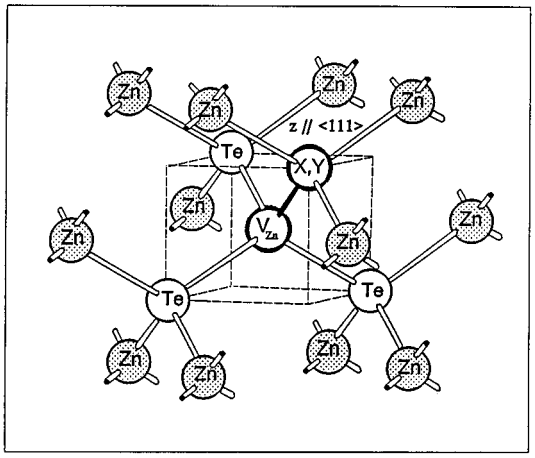

FIG. 8. Microscopic model for the nearest-neighbor pair defects $V_{Zn}^{2+}-Y_{Te}$ and $V_{Zn}^{3+}-X_{Te}$ having trigonal symmetry.

(7). The total-spin quantum numbers following from (7) are $|S_V-S_X|\leqslant S\leqslant|S_V+S_X|$, separated by

$$E(S)=\tfrac{1}{2}J_{V,X}[S(S+1)-S_V(S_V+1)-S_X(S_X+1)]. \tag{8}$$

Now we have to consider which ground-spin manifolds of the pair constituents can produce an $S=\frac{1}{2}$ total-spin manifold. For the V impurity the most probable charge states are $V_{Zn}^{3+}(A^+)$ or $V_{Zn}^{2+}(A^0)$, yielding an $S_V=1$ or $S_V=\frac{3}{2}$ spin manifold, respectively. In the case of the $S_V=\frac{3}{2}$ manifold of $V_{Zn}^{2+}(A^0)$, the recommended spin for the "X_{Te}" defect is $S_X=1$. In our opinion, an $S_X=1$ defect is less probable for "X_{Te}." More likely should be an $S_X=1/2$ ground state for the defect "X_{Te}," which is necessary if we assume V in its ionized donor state $V_{Zn}^{3+}(A^+)$ with $S_V=1$. Considering that the possible pair-formation mechanism usually based on a Coulomb attraction, we predict an acceptorlike defect for "X_{Te}." In its paramagnetic state, the acceptor has to be occupied by a hole. The ground state of the hole in the trigonal pair symmetry is most likely an effective spin-$\frac{1}{2}$ manifold. Therefore, we assume a $V_{Zn}^{3+}-X_{Te}$ pair, where the defect "X_{Te}" has an $S=\frac{1}{2}$ ground state. In the frame of this model using Eq. (8), we get two total-spin levels with $S=\frac{1}{2}$ and $S=\frac{3}{2}$. In the strong isotropic exchange limit, the energy separation between the two levels is much larger than $h\nu$ and zero-field splitting. The EPR spectra are just the superposition of the spectra observed for the two total-spin states according to their thermal population. The total-spin states can be described by a phenomenological spin Hamiltonian. In the present case, we observe only the $S=\frac{1}{2}$ total-spin state. The following relations between the parameters for the S manifold (determined in the experiment) and the parameters of the individual spin centers and exchange spin-Hamilton parameters are given by Bencini and Gatteschi,[23]

$$\mathbf{g}_S=c_1\mathbf{g}_X+c_2\mathbf{g}_V,$$

$$\mathbf{A}_S=c_1\mathbf{A}_X+c_2\mathbf{A}_V,$$

with

$$\begin{array}{cccccc} S_X & S_V & S & c_1 & c_2 \\ \hline \frac{1}{2} & 1 & \frac{1}{2} & -\frac{1}{3} & \frac{4}{3} \\ & & \frac{3}{2} & \frac{1}{3} & \frac{2}{3} \end{array} , \tag{9}$$

where g_S and A_S are the tensors of total-spin states, while g_V, A_V and g_X, A_X are the tensors of the individual constituents of the pair, V and "X_{Te}," respectively. Because we do not know the parameters of the individual constituents in an isomorphous complex, where in each case the other constituent is diamagnetic, we try to use the parameters from the tetrahedral defects for an estimation. Of course we cannot expect to explain the anisotropy which was observed for the parameters of the pair given in Table III. Furthermore, there is no additional hint on the assumed isolated defect "X_{Te}" in the spectra. The reason might be that it exists only in the pair and/or is only generated by the pairing mechanism. What we know about "X_{Te}" is that it gives no measurable contribution to the hyperfine splitting of the pair, therefore, we assumed $I_X=0$. Using the known parameters of the isolated $V_{Zn}{}^{3+}(A^+)$ with $g_V=1.959$, $A_V=57.6\times10^{-4}$ cm^{-1} and the hypothetical parameters for "X_{Te}" with $g=2$ and $I=0$ (that means A_X is not relevant), we get from Eq. (9) for the $S=\frac{1}{2}$ state $g_{1/2}\approx1.97$ and $A_{1/2}\approx76\times10^{-4}$ cm^{-1}. The g value agrees with the experimental ones, but the calculated hyperfine-coupling constant is too large. To get a reasonable value for the hyperfine parameter, the individual V parameter has to be reduced. This conclusion is in plausible accord with the supposition that the electron localization at the V nucleus in the pair has to be lower than in the case of the isolated V defect in tetrahedral symmetry.

In contradiction to our interpretation of the two trigonal spectra by two different pair models, there is the principal possibility that both trigonal spectra, interpreted by $S=\frac{1}{2}$ ($V_{Zn}{}^{3+}-X_{\mathrm{Te}}$) and by $S=\frac{3}{2}$ ($V_{Zn}{}^{2+}-Y_{\mathrm{Te}}$), belong to the same pair characterized by a strong exchange coupling as it was applied for the interpretation of the $S=\frac{1}{2}$ spectrum given in Sec. III B. In this case, the $S=\frac{1}{2}$ and $S=\frac{3}{2}$ spectra would belong to the two total-spin states of the pair. There are two arguments which led us to exclude this possibility of interpretation: First, the temperature dependences of the intensities of both spectra show a typical ground state behavior, which contradicts the fact that one of the spin states ought to be an excited state and second, the ratio of the hyperfine parameters of both spectra is about 1, which is far from the ratio of $A_{1/2}/A_{3/2}=2$ calculated after Eq. (9).

IV. CONCLUSIONS

The optical studies with ZnTe:V have substantiated the occurrence of three charge states of an isolated V impurity: the positively charged $V_{Zn}{}^{3+}(A^+)$, the neutral $V_{Zn}{}^{2+}(A^0)$, and the negatively charged $V_{Zn}{}^{+}(A^-)$. Further luminescence peaks were attributed to V-related pairs or complexes.[(part I)]

Two of the charge states of the isolated V impurity as characterized by luminescence in part I are also verified by EPR, the positively charged $V_{Zn}{}^{3+}(A^+)$, and the neutral $V_{Zn}{}^{2+}(A^0)$ ion in the dark. Therefore, we conclude that the Fermi level is pinned at the V^{3+}/V^{2+} donor level, as it is expected for ZnTe that is usually a p-type material under the applied growing conditions. We could not find any hint on a $V_{Zn}{}^{+}(A^-)$ EPR spectrum, not even under illumination of the sample. The reason might be either that the $V_{Zn}{}^{+}(A^-)$ concentration achievable by illumination is not large enough for an EPR detection or that the resulting ground-state behavior does not allow EPR transitions. Indeed, we expect low transition probabilities for the most probable ground-state behavior of $V_{Zn}{}^{+}(A^-)$ $\{3d^4\}$. $V_{Zn}{}^{+}(A^-)$ has a $^5T_2$ ground state in T_d symmetry that is lowered by JT effect to an orbital doublet and an orbital singlet with $S=2$. The spin degeneracy of the $S=2$ orbital singlet is partly lifted, preferentially by spin-orbit interaction (see the description of the isoelectronic state of Cr^{2+} in II-VI materials[24]). If the yielded fine-structure splitting in an axially distorted crystal field is large compared to the Zeeman splitting, the possible EPR transitions within the doublets have zero or very low transition probabilities.

The EPR spectra, which could be unambiguously assigned to the isolated $V_{Zn}{}^{3+}(A^+)$ in ZnTe, reveal the typical behavior of a the expected $^3A_2$ ground state. The analysis of the resolved Te-ligand hyperfine interaction combined with the commonly accepted assumption that transition metals preferentially occupy lattice sites, suggest that V is incorporated at a Zn cation sites. From analogy to the isoelectronic Cr^{3+} in GaAs, we attribute the triclinic V spectra to the isolated $V_{Zn}{}^{2+}(A^0)$. The origin of the triclinic distortion of the cubic crystal field (T_d) in the ground state should be a static JT effect (an orthorhombic distortion is produced by the interaction of the $^4T_1$ electronic state with ϵ and τ_2 vibrational modes) combined with an additional off-center position. The spectra have been described by a resulting orbital singlet with $S=\frac{3}{2}$. The additional splitting of the ground state could not be verified by the luminescence investigations.

Two additionally observed EPR spectra were assigned to nearest-neighbor V-related defect pairs (Fig. 8). The spectrum of the first one, $V_{Zn}{}^{2+}-Y_{\mathrm{Te}}$, shows trigonal symmetry and can be explained by the $S=\frac{3}{2}$ manifold of an orbital-singlet ground state. The associated defect "Y_{Te}" is responsible for the trigonal distortion of the tetrahedral crystal field of $V_{Zn}{}^{2+}$. This distortion lifts the orbital degeneracy of the $^4T_1$ ground state in T_d symmetry. The spectrum of the second pair defect indicates trigonal symmetry as well and could be described by $S=\frac{1}{2}$. The interpretation of the $S=\frac{1}{2}$ ground-state manifold led us to conclude that a $V_{Zn}{}^{3+}-X_{\mathrm{Te}}$ pair is the most probable cause of the spectrum. Both constituents of the pair should be paramagnetic. The $S=\frac{1}{2}$ ground state is produced by a dominating isotropic exchange interaction, being antiferromagnetic between the $S=1$ ground-state manifold of $V_{Zn}{}^{3+}$ and an assumed $S=\frac{1}{2}$ ground state of "X_{Te}."

In the following, we will discuss some problems of our assignments concerning isolated impurities and pairs. Usually in low or moderately doped II-VI compounds, the concentrations of transition-metal-related complexes are some orders of magnitudes smaller than the concentrations of isolated transition-metal defects. It is surprising that in the present case of V-doped ZnTe four different spectra are observed in the dark, attributed to four different kinds of defects with nearly the same defect concentration. By this fact the assignment of the spectra to isolated defects or to complexes becomes more difficult, especially in the case of the two $S=\frac{3}{2}$ spectra in trigonal and triclinic symmetry. As mentioned in Sec. III A, the main argument for the assignment of the triclinic $V_{Zn}{}^{2+}(A^0)$ defect to the isolated one undergoing

a static JT effect comes from the temperature dependence and the symmetry analogy to the isoelectronic Cr^{3+} in GaAs (Refs. 9 and 10), but it should be repeated here that the results given for V^{2+} in ZnS (Ref. 8) do not fit these arguments.

We have also considered the possibility that V might be placed at interstitial sites, but this type of incorporation seems to be improbable, because we observe nearly the same strength of hyperfine splitting for all spectra. In contrast, one would expect a larger hyperfine splitting for an interstitial than for a substitutional incorporation.

The nature of the associated defects "Y_{Te}" and "X_{Te}" remains unknown for both pairs, because no hyperfine structure could be observed. The comparatively large concentration of pair defects led us to conclude that a donor-acceptor pairing mechanism might be responsible driven by the Coulomb attraction between the constituents, as it is observed for many pairs in semiconductor materials. For the observed pair defects, we have found that V acts as a donor. Therefore, most likely unknown acceptors at a Te site in ZnTe, which yield usually the p-type character of this material, are incorporated in the V-related pairs. In general, group-V and group-IV elements are possible candidates. As intrinsic defects at a Te site, we have to consider the Te vacancy or the Zn_{Te} antisite. It is commonly accepted that the Te vacancy acts as a double donor and can, therefore, not perform the required Coulomb attraction, while the Zn_{Te} antisite defect should be acceptorlike. However, it should be underlined that our argument of Coulomb attraction is not unequivocal and another mechanism producing a minimum in total energy can also be responsible as a driving force. In that case, the possible origin of the defect "X_{Te}" and "Y_{Te}" cannot be restricted to acceptors.

In summary, the EPR results at the ground states confirm the optical data concerning the three possible charge states of the isolated V impurity in ZnTe, where V substitutes for the Zn ion. The observed symmetry lower than T_d for the ground state of $V_{Zn}{}^{2+}(A^0)$ is caused by a JT effect. The reason for the lack of a $V_{Zn}{}^{+}(A^-)$ EPR spectrum might be either that the $V_{Zn}{}^{+}(A^-)$ concentration achievable by illumination is not large enough for an EPR detection and/or that the resulting ground-state behavior does not allow EPR transitions. The two V-related pair defects verified by EPR, $V_{Zn}{}^{2+}-Y_{\mathrm{Te}}$ and $V_{Zn}{}^{3+}-X_{\mathrm{Te}}$, possibly correspond to some low intensity no-phonon lines in the emission spectra.

ACKNOWLEDGMENTS

We are greatly indebted to W. Ulrici for valuable hints concerning the Jahn-Teller effect and helpful discussions. The authors thank W. Gehlhoff for encouraging support. M.U.L. was partially supported by a grant of the Deutscher Akademischer Austauschdienst, Bonn.

*Present address: Department of Physics, University of Notre Dame, Notre Dame, IN 46556.

[1] A. M. Glass and J. Strait, in *Photorefractive Materials and their Applications*, edited by P. Günter and J.-P. Hoignard, Topics in Applied Physics Vol. 61 (Springer-Verlag, Berlin, 1988), p. 237.
[2] J. C. Launay, V. Mazoyer, M. Tapiero, J. P. Zielinger, Z. Guellil, Ph. Delaye, and G. Roosen, Appl. Phys. A **55**, 33 (1992).
[3] M. Ziari, W. H. Steier, P. M. Ranon, S. Trivedi, and M. B. Klein, Appl. Phys. Lett. **60**, 1052 (1992).
[4] W. C. Holton, J. Schneider, and T. L. Estle, Phys. Rev. **133**, A1638 (1964).
[5] H. H. Woodbury and G. W. Ludwig, Bull. Am. Phys. Soc. **6**, 118 (1961).
[6] J. Dielman, in *II-VI Semiconducting Compounds*, edited by D. G. Thomas (Benjamin, New York, 1967), p. 199.
[7] H.-J. Schulz and J. Kreissl, Opt. Mater. **4**, 202 (1994).
[8] J. Schneider, B. Dischler, and A. Räuber, Solid State Commun. **5**, 603 (1967).
[9] J. J. Krebs and G. H. Stauss, Phys. Rev. B **15**, 17 (1977).
[10] G. H. Stauss and J. J. Krebs, Phys. Rev. B **22**, 2050 (1980).
[11] M. Bacci, A. Ranfagni, M. P. Fontana, and G. Viliani, Phys. Rev. B **11**, 3052 (1975).
[12] M. Bacci, A. Ranfagni, M. Ceita, and G. Viliani, Phys. Rev. B **12**, 5907 (1975).
[13] P. Christmann, J. Kreissl, D. M. Hofmann, B. K. Meyer, R. Schwarz, and K. W. Benz, J. Cryst. Growth (to be published).
[14] B. Lambert, M. Gauneau, G. Grandpierre, M. Schoisswohl, H. J. von Bardeleben, J. C. Launay, V. Mazoyer, A. Aoudia, E. Rzepka, Y. Marfaing, and R. Triboulet, Opt. Mater. **4**, 267 (1995).
[15] G. Goetz, U. W. Pohl, H.-J. Schulz, and M. Thiede, J. Lumin. **60–61**, 16 (1994).
[16] S. W. Biernacki, G. Roussos, and H.-J. Schulz, J. Phys. C **21**, 5615 (1988).
[17] G. Goetz, U. W. Pohl, and H.-J. Schulz, J. Phys. Condens. Matter **4**, 8253 (1992).
[18] T. L. Estle and W. C. Holton, Phys. Rev. **150**, 159 (1966).
[19] A. Abragam and B. Bleaney, *Electron Paramagnetic Resonance of Transition Ions* (Dover, New York, 1986).
[20] J. C. M. Hennig, J. Liebertz, and R. P. van Stapele, J. Phys. Chem. Solids **18**, 1109 (1967).
[21] A. Abragam and M. H. L. Pryce, Proc. R. Soc. London Ser. A **206**, 173 (1951).
[22] J. Kreissl, W. Gehlhoff, P. Omling, and P. Emanuelsson, Phys. Rev. B **42**, 1731 (1990).
[23] A. Bencini and D. Gatteschi, *EPR of Exchange Coupled Systems* (Springer-Verlag, Berlin, 1990).
[24] J. T. Vallin and G. D. Watkins, Phys. Rev. B **9**, 2051 (1974).